



Contents lists available at ScienceDirect

Journal of Organometallic Chemistry

journal homepage: www.elsevier.com/locate/jorganchem

Communication

Studies of the decomposition of the ethylene hydrophenylation catalyst $\text{TpRu}(\text{CO})(\text{NCMe})\text{Ph}$ Evan E. Joslin ^{a,1}, Bradley A. McKeown ^a, Thomas R. Cundari ^b, T. Brent Gunnoe ^{a,*}^a Department of Chemistry, University of Virginia, Charlottesville, VA 22904, USA^b Center for Advanced Scientific Computing and Modeling (CASCaM), University of North Texas, Denton, TX 76203, USA

ARTICLE INFO

Article history:

Received 27 February 2017

Received in revised form

30 March 2017

Accepted 31 March 2017

Available online xxx

Keywords:

C–H activation

Ethylene

Hydroarylation

Ruthenium

Homogeneous catalysis

ABSTRACT

$\text{TpRu}(\text{CO})(\text{NCMe})\text{Ph}$ is a catalyst for the conversion of benzene and ethylene to ethylbenzene. Previously, the formation of ethylbenzene has been shown to occur through a pathway that involves ethylene coordination to Ru, insertion of ethylene into the Ru–phenyl bond and Ru–mediated benzene C–H activation. The effect of ethylene pressure and catalyst concentration (between 0.2 and 0.01 mol % based on benzene) on the decomposition of $\text{TpRu}(\text{CO})(\text{NCMe})\text{Ph}$ was examined. Studies have shown that there are two competing catalyst deactivation pathways. At higher concentrations of $\text{TpRu}(\text{CO})(\text{NCMe})\text{Ph}$, the dominant deactivation pathway is likely initiated by a binuclear reaction of two Ru complexes that leads to formation of unidentified paramagnetic species. Kinetic studies reveal that this pathway for catalyst decomposition occurs with a second-order rate of $0.007 (1) \text{ M}^{-1} \text{ s}^{-1}$. At lower Ru concentrations, ethylene C–H activation to form the allyl complex $\text{TpRu}(\text{CO})(\eta^3\text{-C}_4\text{H}_7)$ is the predominant deactivation pathway. The effect of ethylene pressure on catalyst decomposition was also examined. At higher ethylene pressure nearly quantitative formation of $\text{TpRu}(\text{CO})(\eta^3\text{-C}_4\text{H}_7)$ was observed.

© 2017 Elsevier B.V. All rights reserved.

1. Introduction

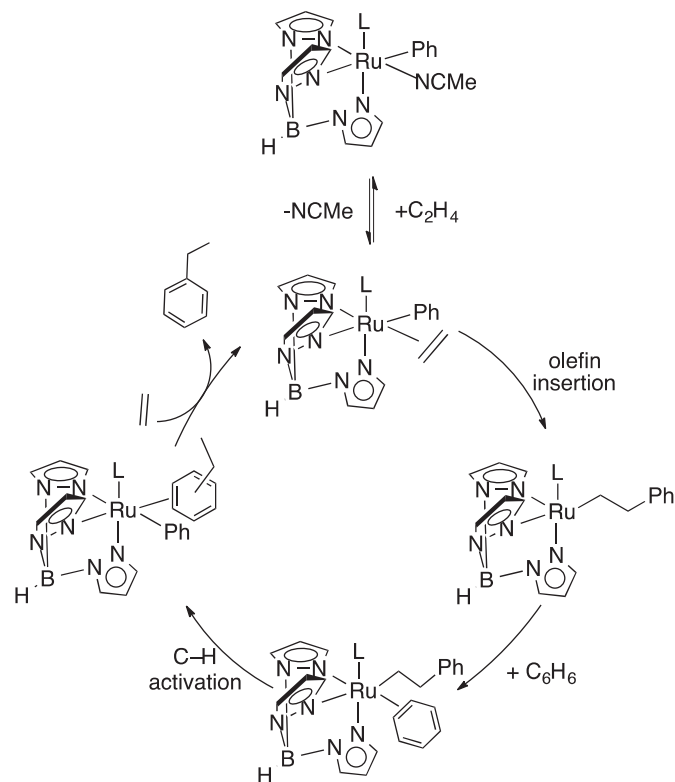
Alkyl arenes traditionally have been synthesized using acid-based catalysts such as Friedel–Crafts catalysts (*i.e.*, a Lewis acid with a Brønsted acid) or using zeolites [1–6]. The use of transition metal catalysts that mediate the same overall process but through a different pathway that involves metal-mediated olefin insertion into metal–aryl bonds and C–H activation provides possible benefits [7–11]. Examples of olefin hydroarylation using simple hydrocarbons, such as benzene and ethylene, are relatively rare [8,12–22]. Our group and others have made progress developing catalysts based on Ir [12,13,23], Pt [14,18–20,24,25], Rh [17,26], and Ru [7,16,27–33] to convert arenes and olefins to alkyl or alkenyl arenes.

Our group has studied ruthenium based catalysts for olefin hydroarylation using $\text{TpRu}(\text{L})(\text{NCMe})\text{Ph}$ (Tp = hydridotris(pyrazolyl) borate; L = CO, PMe_3 , $\text{P}(\text{OCH}_2)_3\text{CEt}$, and 2,6,7-trioxa-1-phosphabicyclo [1,2,2]heptane) complexes [7,27–31]. Through

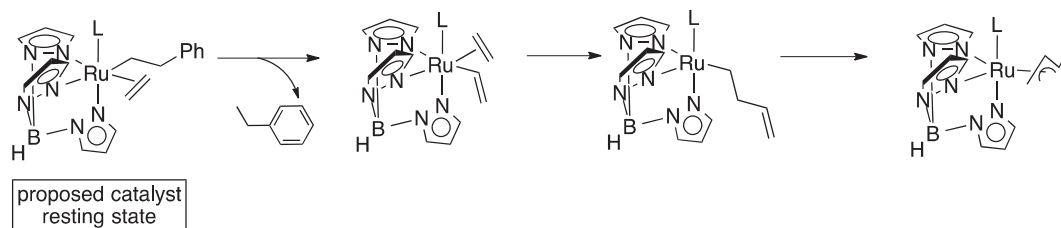
experimental and computational studies, using the hydrophenylation of ethylene to produce ethylbenzene as a model reaction, we have determined that the mechanism for transition metal catalyzed olefin hydroarylation includes two fundamental steps: ethylene insertion into a Ru–Ph bond and benzene C–H activation (Scheme 1) [7]. An important conclusion from our studies of the $\text{TpRu}(\text{L})(\text{NCMe})\text{Ph}$ series is that the ancillary ligand (L) has a significant influence on catalytic performance. For instance, as the ancillary ligand becomes more strongly donating and the Ru(II) center more electron rich (as determined by cyclic voltammetry), the activation barrier for ethylene insertion into the Ru–Ph bond increases. As a result, the rate of ethylene insertion into the Ru–Ph bond is decreased for complexes with more donating L ligands, and ethylene C–H bond activation becomes competitive with catalytic turnover. The net result is that for $\text{TpRu}(\text{L})(\text{NCMe})\text{Ph}$ complexes with L = PMe_3 , $\text{P}(\text{OCH}_2)_3\text{CEt}$, or 2,6,7-trioxa-1-phosphabicyclo [1,2,2]heptane catalyst deactivation occurs rapidly with the formation of $\text{TpRu}(\text{L})(\eta^3\text{-C}_4\text{H}_7)$ complexes (Scheme 2) [7,27–29]. This was also observed to be the mechanism of catalyst deactivation for the cationic Ru(II) catalyst precursor $[(\text{HC}(\text{pz}^5)_3)\text{Ru}(\text{P}(\text{OCH}_2)_3\text{CEt})(\text{NCMe})\text{Ph}][\text{BAR}'_4]$ [$\text{HC}(\text{pz}^5)_3$ = tris(5-methyl-pyrazolyl)methane; BAR'_4 = tetrakis [3,5-bis(trifluoromethyl)phenyl]borate] [16].

* Corresponding author.

E-mail address: tbg7h@virginia.edu (T.B. Gunnoe).¹ Present Address: Department of Chemistry, University of the South: Seawee, Seawee, TN 37383, USA.



Scheme 1. Proposed catalytic cycle for olefin hydroarylation with TpRu(L)(NCMe)Ph complexes.



Scheme 2. Formation of η^3 -methyl allyl through ethylene C–H activation by TpRu complexes.

Thus, we have demonstrated that incorporation of the strongly π -acidic ligand CO (i.e., catalyst precursor TpRu(CO)(NCMe)Ph) gives rise to the longest-lived and most active catalyst among the TpRu(L)(NCMe)Ph series [7,27–32]. Using 0.025 mol % (relative to benzene) of TpRu(CO)(NCMe)Ph at 90 °C and with 0.1 MPa of ethylene, 415 turnovers (TOs) of ethylbenzene were achieved before catalyst deactivation [27]. In contrast, under 0.2 MPa of ethylene in benzene at 90 °C, 0.1 mol % of TpRu(CO)(NCMe)Ph (relative to benzene) catalyzes the formation of ethylbenzene with only approximately 75 TOs of ethylbenzene [31]. Unlike the phosphine and phosphite catalysts, formation of an η^3 -allyl Ru(II) decomposition product was not observed. However, in the absence of benzene, TpRu(CO)(NCMe)Ph and ethylene (1.7 MPa) in THF (70 °C) were demonstrated to convert to $\text{TpRu(CO)(}\eta^3\text{-C}_4\text{H}_7\text{)}$ in nearly quantitative yield [29]. Instead, studies suggest that the deactivation product is a paramagnetic (NMR silent) multinuclear Ru species that could not be definitively characterized [30]. Given the performance of TpRu(CO)(NCMe)Ph and the apparent departure in pathway for catalyst deactivation, we more closely studied the decomposition of TpRu(CO)(NCMe)Ph during catalytic ethylene hydrophenylation. We have found two competing pathways for

catalyst deactivation that are dependent on the reaction conditions.

2. Results and discussion

2.1. Study of TpRu(CO)(NCMe)Ph concentration

To further investigate the disparity between the catalytic results for TpRu(CO)(NCMe)Ph using 0.1 and 0.025 mol % catalyst loadings, a systematic screening of catalyst loading (0.2–0.01 mol % relative to benzene) was performed. Data are shown in Fig. 1. Using a catalyst loading of 0.2 mol % TpRu(CO)(NCMe)Ph , under 0.1 MPa of ethylene at 90 °C catalytic ethylene hydrophenylation results in only 90 TOs of ethylbenzene. Ethylbenzene production increases by more than 5-fold when the catalyst loading is decreased to 0.01 mol % to give 490 TOs.

For the reactions shown in Fig. 1, we probed for the formation of the allyl complex $\text{TpRu(CO)(}\eta^3\text{-C}_4\text{H}_7\text{)}$. After cessation of catalyst activity using 0.2 mol % TpRu(CO)(NCMe)Ph , analysis of the non-volatiles of the reaction by ^1H NMR spectroscopy revealed isolation of $\text{TpRu(CO)(}\eta^3\text{-C}_4\text{H}_7\text{)}$ in 12% yield based on HMDS (hexamethyldisiloxane) as an internal standard. The yield of $\text{TpRu(CO)(}\eta^3\text{-C}_4\text{H}_7\text{)}$ increases with decreased starting catalyst loading (Table 1). This suggests that a competition exists between deactivation pathways to form the previously proposed NMR silent paramagnetic multinuclear Ru species and $\text{TpRu(CO)(}\eta^3\text{-C}_4\text{H}_7\text{)}$ (Scheme 3) [30]. As the starting catalyst concentration is decreased, the deactivation pathway to form $\text{TpRu(CO)(}\eta^3\text{-C}_4\text{H}_7\text{)}$ becomes increasingly competitive.

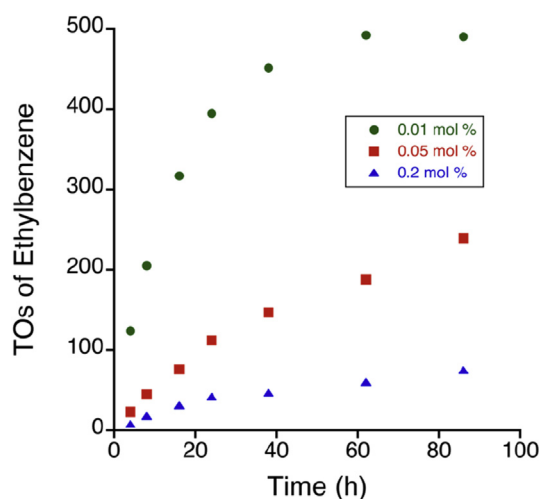


Fig. 1. Comparison of catalytic hydrophenylation of ethylene by TpRu(CO)Ph(NCMe) at 0.1 MPa ethylene and 90 °C at Ru mol % loadings of 0.01, 0.05, and 0.2 mol % (relative to benzene).

Table 1
Effect of catalyst loading on TOs of ethylbenzene and % yield of $\text{TpRu}(\text{CO})(\eta^3\text{-C}_4\text{H}_7)$.^a

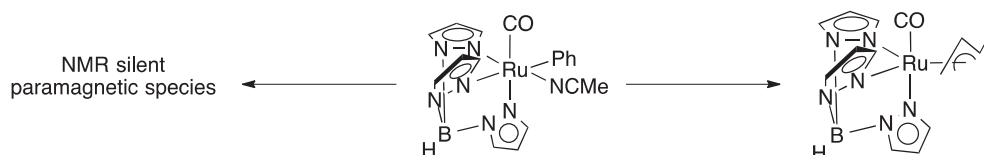
[Ru] (mol %)	TOs ^b	$\text{TpRu}(\text{CO})(\eta^3\text{-C}_4\text{H}_7)$ (% yield) ^c
0.2	90	12
0.1	193	22
0.025	415	60
0.01	490	62

^a Reactions conducted at 0.1 MPa of ethylene in benzene at 90 °C.

^b TOs were determined by GC-MS using *n*-decane as an internal standard.

^c % yield was determined by post catalysis analysis of reaction non-volatiles by ¹H NMR spectroscopy.

$\text{TpRu}(\text{CO})(\text{NCMe})\text{Ph}$ (0.03 M) in $\text{THF-}d_8$ at 75 °C results in slow decomposition of the catalyst precursor as observed by ¹H NMR spectroscopy. As the reaction progresses, resonances for $\text{TpRu}(\text{CO})(\text{NCMe})\text{Ph}$ steadily decrease as very broad resonances consistent with the formation of paramagnetic species appear. Plots of concentration of $\text{TpRu}(\text{CO})(\text{NCMe})\text{Ph}$ and $\ln [\text{TpRu}(\text{CO})(\text{NCMe})\text{Ph}]$ are not linear. However, a second-order plot, $[\text{TpRu}(\text{CO})(\text{NCMe})\text{Ph}]^{-1}$ vs. time, provides a clean linear fit, indicating that the decomposition pathway is likely second order in $\text{TpRu}(\text{CO})(\text{NCMe})\text{Ph}$ (Fig. 3). The rate of decomposition was determined to be $0.007 (1) \text{ M}^{-1} \text{ s}^{-1}$ at 75 °C.



Scheme 3. Competing deactivation pathways during catalytic ethylene hydrophenylation using $\text{TpRu}(\text{CO})(\text{NCMe})\text{Ph}$.

2.2. Influence of ethylene concentration on $\text{TpRu}(\text{CO})(\text{NCMe})\text{Ph}$ decomposition

Previously, it has been demonstrated that the rate of ethylene hydrophenylation catalyzed by $\text{TpRu}(\text{CO})(\text{NCMe})\text{Ph}$ has an inverse dependence on ethylene concentration [31]. The decreased rate of catalysis with increasing ethylene concentration is attributed to the proposed catalyst resting state, $\text{TpRu}(\text{CO})(\eta^2\text{-C}_2\text{H}_4)$ ($\text{CH}_2\text{CH}_2\text{Ph}$), which removes Ru from the catalytic cycle (Scheme 2). Thus, for optimal catalysis, the ethylene to benzene ratio is required to be low. We anticipated that the pathway of deactivation of $\text{TpRu}(\text{CO})(\text{NCMe})\text{Ph}$ might depend on ethylene concentration. To examine the effect of ethylene concentration on catalyst deactivation, catalytic experiments were conducted using 0.01 mol % $\text{TpRu}(\text{CO})(\text{NCMe})\text{Ph}$ (relative to benzene) at 90 °C with varied ethylene pressures (0.1, 0.2 or 0.3 MPa).

Catalytic reactions with 0.01 mol % $\text{TpRu}(\text{CO})(\text{NCMe})\text{Ph}$ and 0.1 MPa of ethylene in benzene achieve 490 TOs of ethylbenzene after c.a. (or approximately) 60 h at 90 °C. Analysis of the reaction non-volatiles after catalyst deactivation by ¹H NMR spectroscopy showed formation of $\text{TpRu}(\text{CO})(\eta^3\text{-C}_4\text{H}_7)$ in 62% yield. As the ethylene pressure is increased, catalytic activity and longevity are significantly reduced (Fig. 2). For example, increasing the ethylene pressure to 0.3 MPa results in an ~80% decrease in TOs with no observed catalytic activity after 12 h of reaction. This is attributed to an increase in the rate of $\text{TpRu}(\text{CO})(\eta^3\text{-C}_4\text{H}_7)$ formation at higher ethylene concentration in solution. At ethylene pressures ≥ 0.1 MPa, the formation of the allyl complex, $\text{TpRu}(\text{CO})(\eta^3\text{-C}_4\text{H}_7)$, is quantitative (Table 2). These results suggest that at low ethylene concentrations, deactivation via formation of $\text{TpRu}(\text{CO})(\eta^3\text{-C}_4\text{H}_7)$ is competitive with formation of the proposed paramagnetic complex (the formation of which is presumed to be independent of ethylene; see below), but the allyl complex dominates at higher ethylene concentrations.

2.3. Kinetics of $\text{TpRu}(\text{CO})(\text{NCMe})\text{Ph}$ decomposition under non-catalytic conditions

Probing the deactivation of $\text{TpRu}(\text{CO})(\text{NCMe})\text{Ph}$ under catalytic conditions (i.e., in the presence of benzene and ethylene) is complicated by the two proposed competing processes (Scheme 3). Thus, we studied the decomposition of $\text{TpRu}(\text{CO})(\text{NCMe})\text{Ph}$ in the absence of benzene and ethylene. Heating a solution of

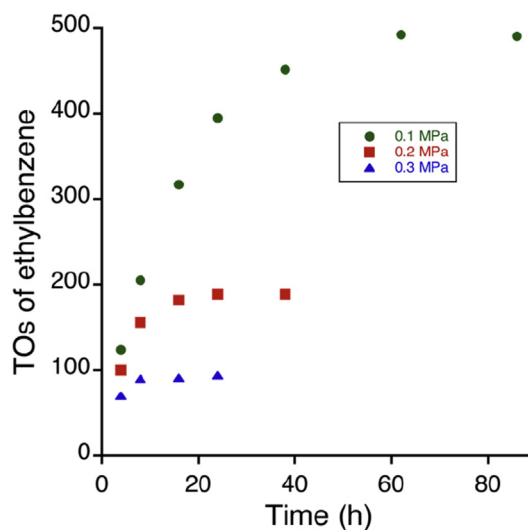


Fig. 2. Comparison of ethylene hydrophenylation at various pressures of ethylene using $\text{TpRu}(\text{CO})(\text{NCMe})\text{Ph}$ (0.01 mol % relative to benzene) as the catalyst precursor at 90 °C.

Table 2
Comparison of $\text{TpRu}(\text{CO})(\eta^3\text{-C}_4\text{H}_7)$ yield from catalytic ethylene hydrophenylation with variable ethylene pressure.^a

Ethylene pressure (MPa)	Time (h)	TOs ^b	$\text{TpRu}(\text{CO})(\eta^3\text{-C}_4\text{H}_7)$ (% yield) ^c
0.1	62	490	62
0.2	16	189	Quantitative
0.3	8	94	Quantitative

^a 0.01 mol % $\text{TpRu}(\text{CO})(\text{NCMe})\text{Ph}$ at 90 °C.

^b TOs was determined by GC-MS using *n*-decane, as an internal standard.

^c % yield was determined by post catalysis analysis of reaction non-volatiles by ¹H NMR spectroscopy.

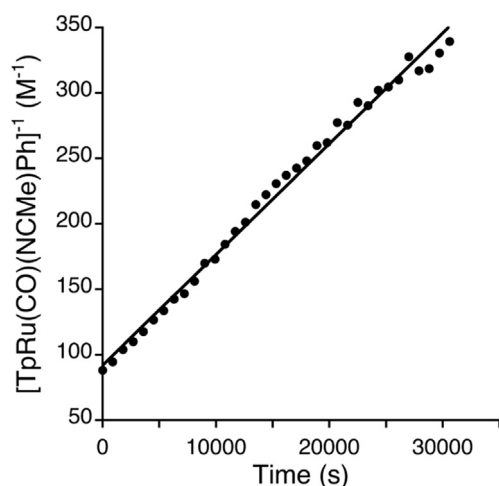


Fig. 3. Second-order plot for the decomposition of $\text{TpRu}(\text{CO})(\text{NCMe})\text{Ph}$ in $\text{THF-}d_8$ at $75\text{ }^\circ\text{C}$, as monitored by ^1H NMR spectroscopy ($R^2 = 0.98$).

3. Conclusions

$\text{TpRu}(\text{CO})(\text{NCMe})\text{Ph}$ is an effective catalyst for ethylene hydrophenylation. In an effort to better understand possible pathways for catalyst deactivation, the influence of catalyst loading and ethylene pressure on catalytic performance and deactivation product was examined. Based on these studies, there are two competing deactivation pathways for catalytic ethylene hydrophenylation: 1) a likely bimolecular decomposition pathway that results in the formation of uncharacterized paramagnetic species, and 2) formation of the η^3 -allyl complex $\text{TpRu}(\text{CO})(\eta^3\text{-C}_4\text{H}_7)$, which arises due to ethylene C–H activation (Scheme 2). It was determined that both the starting catalyst precursor and ethylene concentration influence catalyst longevity as well as the dominant pathway for deactivation. Higher catalyst loading and low ethylene concentrations bias the decomposition toward the formation of paramagnetic species, while low catalyst loading and high ethylene concentrations result in formation of $\text{TpRu}(\text{CO})(\eta^3\text{-C}_4\text{H}_7)$. Optimal catalytic conditions for maximum turnovers were found to be with low catalyst loadings and ethylene concentrations.

4. Materials and methods

4.1. General methods

Unless otherwise noted, all synthetic procedures were performed under anaerobic conditions in a nitrogen-filled glovebox or by using standard Schlenk techniques. Glovebox purity was maintained by periodic nitrogen purges and was monitored by an oxygen analyzer [$\text{O}_2(\text{g}) < 15\text{ ppm}$ for all reactions]. The preparation, isolation and characterization of $\text{TpRu}(\text{CO})\text{Ph}(\text{NCMe})$ [31] and $\text{TpRu}(\text{CO})(\eta^3\text{-C}_4\text{H}_7)$ [29] have been previously reported. Benzene was purified by passage through a column of activated alumina. Benzene- d_6 and THF- d_8 were stored under a nitrogen atmosphere over 4 \AA molecular sieves. ^1H NMR spectra were recorded on a Varian MRS 600 MHz spectrometer. All ^1H spectra are referenced against residual proton signals. GC/MS was performed using a Shimadzu GCMS-QP2010 Plus system with simulated electron impact or electron impact ionization. Ethylene (99.5%) was purchased from GTS-Welco and used as received. All other reagents were used as received from commercial sources.

4.2. Representative catalytic ethylene hydrophenylation reaction

$\text{TpRu}(\text{CO})(\text{NCMe})\text{Ph}$ (0.0103 g, 0.0224 mmol, 0.1 mol % Ru relative to benzene) was dissolved in 2 mL of benzene. In a 25 mL volumetric flask, *n*-decane (0.199 g, 0.273 mL, 0.5 mol % *n*-decane relative to benzene) was added to benzene to produce a stock solution containing an internal standard. To generate 6 mL of a 0.025 mol % Ru catalyst solution: 1.5 mL of a 0.1 mol % Ru solution, 1.5 mL of a 0.5 mol % *n*-decane solution and 3 mL of benzene were transferred to a stainless steel pressure reactor. The reactor was charged with 0.1 MPa of ethylene, pressurized with dinitrogen to a total pressure of 0.8 MPa, and heated to $90\text{ }^\circ\text{C}$. After a given duration of time the reactor was cooled to room temperature and an aliquot of the reaction mixture was removed. The reaction mixture was analyzed by GC/MS using peak areas of the products and the internal standard to calculate product yields. Ethylbenzene production was quantified using linear regression analysis of gas chromatograms of standard samples. A set of eight known standards were prepared consisting of 1:5, 3:5, 5:5, 7.5:5, 10:5, 50:5, 100:5 and 150:5 M ratios of ethylbenzene to *n*-decane in methylene chloride. A plot of peak area ratios versus molar ratios gave a regression line. For the GC/MS system, the slope and correlation coefficient for ethylbenzene were 0.18 and 0.99, respectively. All reactions were repeated in triplicate to ensure reproducibility.

4.3. Quantification of $\text{TpRu}(\text{CO})(\eta^3\text{-C}_4\text{H}_7)$ from catalytic experiments

A catalytic reaction was performed as stated above. After completion of catalysis, the reactor was brought into the glovebox, and the volatiles were removed *in vacuo*. The non-volatiles were dissolved in C_6D_6 (0.4 mL) and placed in an NMR tube with 20 μL of a 5.0 mM HMDS (hexamethyldisiloxane) stock solution in C_6D_6 . A ^1H NMR spectrum was collected (pulse delay of 20 s) and an allyl resonance corresponding to $\text{TpRu}(\text{CO})(\eta^3\text{-C}_4\text{H}_7)$ (4.4 ppm) was integrated relative to the HMDS standard to calculate the percent yield of $\text{TpRu}(\text{CO})(\eta^3\text{-C}_4\text{H}_7)$.

4.4. Kinetic measurements of $\text{TpRu}(\text{CO})(\text{NCMe})\text{Ph}$ decomposition

A THF- d_8 solution of $\text{TpRu}(\text{CO})(\text{NCMe})\text{Ph}$ (0.0125 g, 0.0272 mmol) and hexamethyldisilane (as an internal standard) was made in a 1 mL volumetric flask. The solution was divided (300 μL aliquots) and transferred into three J. Young NMR tubes. The NMR tubes were placed into the temperature calibrated NMR probe (equilibrated at $76\text{ }^\circ\text{C}$). The temperature was determined using a 80% Ethylene Glycol in DMSO- d_6 and the following equation provided by Bruker Instruments, Inc. VT-Calibration Manual: $T(\text{K}) = (4.218 - \Delta)/0.009132$, where Δ is the shift difference (ppm) between CH_2 and OH peaks of the ethylene glycol. Reaction progress was monitored by ^1H NMR spectroscopy using automated data acquisition. A single transient was used for each time point with 900 s delay between transients. The rate of the reaction was determined by monitoring the disappearance of the most upfield Tp resonance (6.02 ppm) of the starting material. The rate of decomposition was determined utilizing data up to 75% conversion (30,000 s), as the presence of a significant concentration of the resultant paramagnetic product introduced substantial error in the resonance integrations.

Funding

We thank the U.S. Department of Energy, Office of Basic Energy Sciences, Division of Chemical Sciences, Geosciences, and Biosciences for support of this research via grants DE-SC0000776

(T.B.G.) and DE-FG02-03ER15387 (T.R.C.).

References

- [1] C. Perego, P. Pollesel, in: E. Stefan (Ed.), *Adv. Nanoporous Mater*, Elsevier, 2010, pp. 97–149.
- [2] A. Corma, *Chem. Rev.* 97 (1997) 2373–2420.
- [3] C. Perego, P. Ingallina, *Catal. Today* 73 (2002) 3–22.
- [4] G.A. Olah, A. Molnar, *Hydrocarbon Chemistry*, second ed., Wiley-Interscience, New York, 2003.
- [5] R.M. Roberts, A.A. Khalaf, *Friedel-Crafts Alkylation Chemistry: a Century of Discovery*, Marcel Dekker, Inc., New York, 1984.
- [6] J.A. Kocal, B.V. Vora, T. Imai, *Appl. Catal. A* 221 (2001) 295–301.
- [7] N.A. Foley, J.P. Lee, Z.F. Ke, T.B. Gunnoe, T.R. Cundari, *Acc. Chem. Res.* 42 (2009) 585–597.
- [8] J.R. Andreatta, B.A. McKeown, T.B. Gunnoe, *J. Organomet. Chem.* 696 (2011) 305–315.
- [9] C.G. Jia, T. Kitamura, Y. Fujiwara, *Acc. Chem. Res.* 34 (2001) 633–639.
- [10] F. Kakiuchi, S. Murai, *Acc. Chem. Res.* 35 (2002) 826–834.
- [11] V. Ritleng, C. Sirlin, M. Pfeffer, *Chem. Rev.* 102 (2002) 1731–1769.
- [12] J. Oxgaard, R.A. Periana, W.A. Goddard, *J. Am. Chem. Soc.* 126 (2004) 11658–11665.
- [13] J. Oxgaard, R.P. Muller, W.A. Goddard, R.A. Periana, *J. Am. Chem. Soc.* 126 (2004) 352–363.
- [14] M.A. Bowring, R.G. Bergman, T.D. Tilley, *Organometallics* 30 (2011) 1295–1298.
- [15] A.T. Luedtke, K.I. Goldberg, *Angew. Chem. Int. Ed.* 47 (2008) 7694–7696.
- [16] S.A. Burgess, E.E. Joslin, T.B. Gunnoe, T.R. Cundari, M. Sabat, W.H. Myers, *Chem. Sci.* 5 (2014) 4355–4366.
- [17] B.A. Vaughan, M.S. Webster-Gardiner, T.R. Cundari, T.B. Gunnoe, *Science* 348 (2015) 421–424.
- [18] S. Pal, S. Kusumoto, K. Nozaki, *Organometallics* 36 (2017) 502–505.
- [19] M.L. Clement, K.A. Grice, A.T. Luedtke, W. Kaminsky, K.I. Goldberg, *Chem. - Eur. J.* 20 (2014) 17287–17291.
- [20] B.A. McKeown, H.E. Gonzalez, M.R. Friedfeld, T.B. Gunnoe, T.R. Cundari, M. Sabat, *J. Am. Chem. Soc.* 133 (2011) 19131–19152.
- [21] L.A. Goj, T.B. Gunnoe, *Curr. Org. Chem.* 9 (2005) 671–685.
- [22] T. Matsumoto, *Catal. Surv. Asia* 11 (2007) 31–48.
- [23] T. Matsumoto, D.J. Taube, R.A. Periana, H. Taube, H. Yoshida, *J. Am. Chem. Soc.* 122 (2000) 7414–7415.
- [24] B.A. McKeown, J.P. Lee, J. Mei, T.R. Cundari, T.B. Gunnoe, *Eur. J. Inorg. Chem.* 2016 (2016) 2296–2311.
- [25] B.A. McKeown, N.A. Foley, J.P. Lee, T.B. Gunnoe, *Organometallics* 27 (2008) 4031–4033.
- [26] B.A. Vaughan, S.K. Khani, J.B. Gary, J.D. Kammert, M.S. Webster-Gardiner, B.A. McKeown, R.J. Davis, T.R. Cundari, T.B. Gunnoe, *J. Am. Chem. Soc.* 139 (2017) 1485–1498.
- [27] E.E. Joslin, C.L. McMullin, T.B. Gunnoe, T.R. Cundari, M. Sabat, W.H. Myers, *Organometallics* 31 (2012) 6851–6860.
- [28] N.A. Foley, Z.F. Ke, T.B. Gunnoe, T.R. Cundari, J.L. Petersen, *Organometallics* 27 (2008) 3007–3017.
- [29] N.A. Foley, M. Lail, J.P. Lee, T.B. Gunnoe, T.R. Cundari, J.L. Petersen, *J. Am. Chem. Soc.* 129 (2007) 6765–6781.
- [30] M. Lail, B.N. Arrowood, T.B. Gunnoe, *J. Am. Chem. Soc.* 125 (2003) 7506–7507.
- [31] M. Lail, C.M. Bell, D. Conner, T.R. Cundari, T.B. Gunnoe, J.L. Petersen, *Organometallics* 23 (2004) 5007–5020.
- [32] N.A. Foley, M. Lail, T.B. Gunnoe, T.R. Cundari, P.D. Boyle, J.L. Petersen, *Organometallics* 26 (2007) 5507–5516.
- [33] H. Weissman, X. Song, D. Milstein, *J. Am. Chem. Soc.* 123 (2001) 337–338.